Molecules and Cells

Inhibitory Role of TRIP-Br1/XIAP in Necroptosis under Nutrient/Serum Starvation

Zolzaya Sandag[1,2], Samil Jung[1,2], Nguyen Thi Ngoc Quynh[1], Davaajargal Myagmarjav[1], Nguyen Hai Anh[1], Dan-Diem Thi Le[1], Beom Suk Lee[1], Raj Kumar Mongre[1], Taeyeon Jo[1], and MyeongSok Lee[1,*]

[1]Department of Biological Science, Sookmyung Women's University, Seoul 14310, Korea, [2]These authors contributed equally to this work.
*Correspondence: mslee@sookmyung.ac.kr
https://doi.org/10.14348/molcells.2020.2193
www.molcells.org

Currently, many available anti-cancer therapies are targeting apoptosis. However, many cancer cells have acquired resistance to apoptosis. To overcome this problem, simultaneous induction of other types of programmed cell death in addition to apoptosis of cancer cells might be an attractive strategy. For this purpose, we initially investigated the inhibitory role of TRIP-Br1/XIAP in necroptosis, a regulated form of necrosis, under nutrient/serum starvation. Our data showed that necroptosis was significantly induced in all tested 9 different types of cancer cell lines in response to prolonged serum starvation. Among them, necroptosis was induced at a relatively lower level in MCF-7 breast cancer line that was highly resistant to apoptosis than that in other cancer cell lines. Interestingly, TRIP-Br1 oncogenic protein level was found to be very high in this cell line. Up-regulated TRIP-Br1 suppressed necroptosis by repressing reactive oxygen species generation. Such suppression of necroptosis was greatly enhanced by XIAP, a potent inhibitor of apoptosis. Our data also showed that TRIP-Br1 increased XIAP phosphorylation at serine87, an active form of XIAP. Our mitochondrial fractionation data revealed that TRIP-Br1 protein level was greatly increased in the mitochondria upon serum starvation. It suppressed the export of CypD, a vital regulator in mitochondria-mediated necroptosis, from mitochondria to cytosol. TRIP-Br1 also suppressed shikonin-mediated necroptosis, but not TNF-α-mediated necroptosis, implying possible presence of another signaling pathway in necroptosis. Taken together, our results suggest that TRIP-Br1/XIAP can function as onco-proteins by suppressing necroptosis of cancer cells under nutrient/serum starvation.

Keywords: necroptosis, programmed cell death, TRIP-Br1, XIAP

INTRODUCTION

Cancer is still considered as one of the leading causes of morbidity and mortality worldwide despite advances in the field of anti-cancer drug discovery and development (Ferlay et al., 2015). Among many characteristics of cancer cells, the ability of cancer cells to evade cell death is one of the biggest obstacles in cancer therapies (Hanahan and Weinberg, 2011). Over the past few decades, apoptosis has been targeted mainly to kill cancer cells. Therefore, many currently available anti-cancer drugs are designed to activate the apoptotic pathway either directly or indirectly. However, many cancer cells have acquired resistance to apoptosis via induction of defective apoptotic machinery (e.g., absence of caspase 3) or overexpression of pro-survival proteins, which is a major problem of traditional chemotherapy. Therefore, it is very important to establish new therapies that target different forms of cell death aside from apoptosis.

Cell death has been primarily divided into two types:

Received 27 August 2019; revised 19 December 2019; accepted 2 January 2020; published online 13 February, 2020

eISSN: 0219-1032
©The Korean Society for Molecular and Cellular Biology. All rights reserved.
This is an open-access article distributed under the terms of the Creative Commons Attribution-NonCommercial-ShareAlike 3.0 Unported License. To view a copy of this license, visit http://creativecommons.org/licenses/by-nc-sa/3.0/.

apoptosis (regulated and programmed cell death [PCD]) and necrosis (unregulated and accidental cell death) for a long time. However, recent studies have ushered in overwhelming in the concept of cell death (Nikoletopoulou et al., 2013; Su et al., 2015; Xu et al., 2016). For example, necrosis is now considered a type of PCD (Belizário et al., 2015; Berghe et al., 2014; Cai et al., 2014; Chan et al., 2015; Christofferson and Yuan, 2010; Dasgupta et al., 2017; De Almagro and Vucic, 2015; Dondelinger et al., 2016; Eigenbrod et al., 2008; Fulda, 2013; González-Juarbe et al., 2015; He et al., 2009; Jouan-Lanhouet et al., 2014; Kaczmarek et al., 2013; Moriwaki et al., 2015; Pasparakis and Vandenabeele, 2015; Teng et al., 2005; Vandenabeele et al., 2010; Wang et al., 2014). Accordingly, it is designated as necroptosis, apoptosis-like necrosis, to distinguish it from passive necrosis (Teng et al., 2005). We have tried to find anti-cancer drugs or stresses that can trigger necroptosis as well as apoptosis, especially in apoptosis-resistant cancer cells. Toward this end, it is important to understand both apoptosis and necroptosis, which are mediated via similar but unique signaling pathways depending on the types of stress and stimuli.

Apoptosis is a caspase-dependent PCD that is mediated by either extrinsic or intrinsic pathways via activation of caspases. The extrinsic pathway is activated by various death receptor-ligand interactions. Upon ligand binding to death receptors, the cytoplasmic death domains attract adaptor molecules and eventually lead to activation of caspase-8 which in turn activates downstream caspases. The intrinsic mitochondrial pathway is regulated by Bcl-2 family proteins that control mitochondrial membrane permeability (MMP). Cytochrome C is released from the outside of the inner mitochondrial membrane into cytosol. It binds to apoptotic protease activating factor (Apaf1) and forms the apoptosome complex. Apoptosome activates caspase-9 which in turn activates the downstream elements of caspase cascade (e.g. caspase-3). Apoptosis is morphologically characterized by rounding up of cells, chromatic condensation, nuclear fragmentation, and shedding of apoptotic bodies.

Necroptosis is a caspase-independent form of cell death unlike apoptosis. Necroptosis can be induced by upstream cell death receptors such as the tumor necrosis factor (TNF) receptor superfamily, T-cell receptors (TCR), interferon receptors (IFNs), and Toll-like receptors (TLRs) (Chan et al., 2015; Dondelinger et al., 2016; Fulda, 2013; Nikoletopoulou et al., 2013; Su et al., 2015). TNF-α-mediated necroptosis is the most well-studied signaling pathway inducing necroptosis, which is mainly mediated via activation of three main core regulators: receptor-interacting protein 1 (RIP1) kinase, receptor-interacting protein 3 (RIP3), and mixed lineage kinase domain-like protein (MLKL) (De Almagro and Vucic, 2015; Berghe et al., 2014; He et al., 2009; Moriwaki et al., 2015; Wang et al., 2014). RIP1 is known to mediate both apoptosis and necroptosis, while RIP3 and MLKL are necroptosis specific kinase and actual executer required for necrosome formation, respectively. They form three different types of complexes (membrane-bound complex I, complex II, and necrosome) sequentially by changing the binding partners (Berghe et al., 2014; Cai et al., 2014; De Almagro and Vucic, 2015; He et al., 2009; Moriwaki et al., 2015; Wang et al., 2014). The mechanism entails RIP1 phosphorylation of RIP3, which triggers MLKL phosphorylation and induces necrotic plasma membrane permeabilization (Cai et al., 2014). The RIP1–RIP3–MLKL-dependent necroptosis is now considered a primary mechanism mediating the suppression of tumorigenesis and progression. Cancer cells may suppress necroptosis by down-regulating or inducing functional mutations in RIP1, RIP3, and MLKL. Unlike apoptosis, necroptosis induces inflammation by releasing damage associated molecular patterns (DAMPs), IL-1 family cytokines, nuclear high mobility group box-1 proteins (HMBG1), and cyclophilin A (CypA) (Christofferson and Yuan, 2010; Eigenbrod et al., 2008; Pasparakis and Vandenabeele, 2015). Necroptosis varies morphologically from apoptosis. It results in loss of physical integrity including swelling of organelles, increased cellular volume, disruption of plasma and mitochondrial membranes, and eventual release of intracellular contents.

Necroptosis can be induced by various types of stress including extreme nutrient deficiency (e.g., depletion of glucose, serum, amino acids, and growth factors). Metabolic stress can trigger a set of responses. Initially, nutrient starvation induces autophagy, which contributes to cell survival by supplying additional nutrient and energy to starved cells. However, prolonged starvation eventually results in autophagy-mediated cell death and apoptosis. Severe and extreme starvation ultimately induces necroptosis. Unlike normal cells, cancer cells require very large amounts of nutrients to support uncontrolled growth and proliferation. Thus, they are more susceptible to severe nutrient starvation compared to normal cells. However, many cancer cells have developed tolerance to nutrient limitation by increasing nutrient uptake via changes in metabolic signaling pathways or by activating angiogenesis (Izuishi et al., 2000). Nonetheless, the underlying signaling pathways have yet to be fully elucidated in order to develop novel therapeutic approaches. In this report, we initially focused on nutrient starvation-induced necroptosis as an alternative strategy to treat cancer. To this end, we first studied the inhibitory mechanism of TRIP-Br1 (transcriptional regulator interacting with the PHD-bromodomain 1, also known as SERTAD1/SEI-1/p34^{SEI-1}) and XIAP (X-linked inhibitor of apoptosis protein), which play a key role in response to many different types of cell death.

TRIP-Br1 is known to be involved in various biological processes such as cell cycle, transcriptional regulation, cellular senescence, chromosomal instability, tumorigenesis, and cell death (Hong et al., 2009; 2011; Hsu et al., 2001; Jung et al., 2013; 2014; 2015; Lee et al., 2009; 2015; Li et al., 2015; Sugimoto et al., 1999; Tang et al., 2002; 2005). Many research groups including ours have suggested that TRIP-Br1 is an oncogenic protein, which is overexpressed in several cancer cell lines (Jung et al., 2015; Tang et al., 2002). Our previous study has shown that serum depletion increases TRIP-Br1 protein expression only in cancer cell lines, especially in breast cancer cells, but not in normal cells (Jung et al., 2015). Up-regulated TRIP-Br1 facilitates cancer cell survival by suppressing autophagy-mediated PCD, apoptosis, and necroptosis (Jung et al., 2015). Based on results of our previous study, the present study elucidated the TRIP-Br-mediated mechanism of necroptosis inhibition.

Toward this end, we first focused on XIAP, a central regulator of apoptotic cell death. We have previously reported that TRIP-Br1 inhibits apoptosis by directly binding and stabilizing XIAP (Hong et al., 2009). It is considered as an oncogenic protein and a potent apoptosis inhibitor. It is overexpressed in various malignant cancer cells. A high level of XIAP expression is strongly related to chemotherapy resistance (Berezovskaya et al., 2005; Deveraux et al., 1999; Mizutani et al., 2007; Van Themsche et al., 2009). In addition, XIAP is a key member of IAP protein family. However, it is distinguished from other IAPs due to its strong prevention of cell death induced by various stresses or stimuli (e.g., UV light, genotoxic agents, TNF-α, Fas, etc.) (Duckett et al., 1998). Further, it directly binds and inhibits caspases, unlike other members of the IAP family. XIAP carries three BIR domains that are essential for direct binding to active caspases-9, -3, and -7, which suppresses both intrinsic and extrinsic apoptotic pathways (Chai et al., 2001; Riedl et al., 2001; Shiozaki et al., 2003).

Considering the importance of TRIP-Br1 and XIAP in a diverse range of vital cellular functions, we investigated the mechanism of necroptosis inhibition by TRIP-Br1/XIAP in response to nutrient starvation. This study hypothesized that TRIP-Br1/XIAP is a combined target for efficient killing of cancer cells, especially apoptosis resistant cancer cells, by inducing necroptosis and apoptosis under low-nutrient conditions.

MATERIALS AND METHODS

Cell lines, cell culture, and cell treatment

Each cell line was cultured in one of the following culture media. Four breast cancer cell lines (MCF-7, MDA-MB-231, SKBr3, and HS578T), two lung cancer cell lines (A549 and NCI-H1299), one cervical cancer cell line (HeLa), and one colon cancer cell line (HCT116) were cultured in Dulbecco's modified Eagle's medium (DMEM; WelGENE, Korea) supplemented with 10% fetal bovine serum (FBS) (Gibco, USA) and 1% antibiotic-antimycotic solution (cat. No. 15240-06; Gibco). HT-29 colon cancer cell line was cultured in Roswell Park Memorial Institute (RPMI) 1640 medium (WelGENE) supplemented with 10% FBS and 1% antibiotic-antimycotic solution. All cells were cultured at 37°C in a humidified atmosphere with 95% air and 5% CO_2. Cell morphology was imaged using an optical microscope with IS capture software (KI-400F; Korea Lab Tech, Korea) at ×100 magnification. To induce serum starved conditions, cells were cultured in DMEM and RPMI media without 10% FBS for indicated times. Cell lines were purchased from the American Type Culture Collection (ATCC). Human breast cancer cell lines MCF-7 with wild-type or knock-down TRIP-Br1 were established in our previous study (Jung et al., 2015). Materials used in this study were purchased to prepare the following reagents: 100 ng/ml TNF-α (cat. No. 210-TA; R&D Systems, USA), 100 μM Smac mimetic LCL-161 (cat. No. A11928; AdooQ, USA), 20 μM zVAD-fmk (cat. No. ALX-260-020; Enzo Life Science, USA), and 25-100 μM shikonin (cat. No. 565850; Calbiochem, USA).

Western blotting analysis

Cells were centrifuged (Smart R17; Hanil Scientific, Korea) at 3,000*g* for 3 min at 4°C, washed with ice-cold phosphate-buffered saline (PBS), and lysed in radioimmunoprecipitation assay (RIPA) lysis buffer (50 mM Tris, pH 7.5; 48 mM NaCl; 1% Triton X-100; and 1 mM EGTA) with 0.5 mM Na_3VO_4, 1 mM DTT, and 1 μl pre-made protease inhibitor cocktail III (cat. No. P-1512; AG Scientific, USA) per ml of RIPA buffer. Protein concentration was quantified using a protein assay kit (Bio-Rad Laboratories, USA) followed by loading of 10 to 30 μg protein in each lane of 10% to 12% gels for SDS-PAGE. The separated proteins were electrophoretically transferred onto an Immobilon-P® polyvinylidene fluoride transfer membrane (cat. No. IPVH00010; EMD Millipore, USA). Membranes were blocked with 5% skimmed milk in PBS for 30-60 min at 20-25°C and incubated with primary antibodies at 4°C overnight. After washing with Tris-buffered saline containing 1% Tween 20 (cat. No. T1027; Biosesang, Korea), the membranes were incubated with corresponding secondary antibodies: anti-rabbit (cat. No. 7074S, 1:5,000; Cell Signaling Technology, USA), anti-mouse (cat. No. sc-516102, 1:5,000; Santa Cruz Biotechnology, USA), and anti-goat (cat. No. sc-2020, 1:5,000; Santa Cruz Biotechnology). Immunodetection was performed using a PowerOpti-ECL western blotting detection reagent (cat. No. LR01-02; BioNote, Korea). Antibodies used in this study were as follows: mouse monoclonal anti-TRIP-Br1 (cat. No. ALX-804-645, 1:20,000; Enzo Life Sciences), rabbit polyclonal anti-XIAP (cat. No. 2042, 1:3,000; Cell Signaling Technology, USA), rabbit polyclonal anti-phospho-XIAP (S87) (cat. No. Ab193315, 1:3,000; Abcam, UK), mouse monoclonal anti-BAX (cat. No. sc-7480, 1:3,000; Santa Cruz Biotechnology), rabbit polyclonal anti-Bak (cat. No. 3814S, 1:3,000; Cell Signaling Technology), rabbit polyclonal anti-Bcl-2 (cat. No. 2872, 1:3,000; Cell Signaling Technology), rabbit polyclonal anti-Cytochrome C (cat. No. sc-7159, 1:3,000; Santa Cruz Biotechnology), rabbit polyclonal anti-cyclophilin A (CypA) (cat. No. BML-SA296, 1:1,000; Enzo Life Sciences), mouse monoclonal anti-CypD (cat. No. ab110324, 1:3,000; Abcam), goat- polyclonal anti-RIP3 (cat. No. Sc-47368, 1:3,000; Santa Cruz Biotechnology), rabbit monoclonal anti-pRIP3(S227) (cat. No. Ab209384, 1:3,000; Abcam), rabbit monoclonal anti-MLKL (cat. No. Ab184718, 1:3,000; Abcam), rabbit monoclonal anti-phospho-MLKL (S358) (cat. No. ab187091, 1:3,000; Abcam), rabbit monoclonal anti-Drp1 (cat. No. 5391, 1:3,000; Cell Signaling Technology), rabbit polyclonal anti-HSP60 (cat. No. sc-139661, 1:3,000; Santa Cruz Biotechnology), and mouse monoclonal anti-β-actin (cat. No. sc-47778, 1:5,000; Santa Cruz Biotechnology). β-Actin was used as a loading control. Results of western blot analysis were semi-quantified using ImageJ software (ver. 1.51u; National Institutes of Health, USA). Relative intensity was compared to β-actin and presented in bar graphs.

Analysis of necroptosis and apoptosis

Necroptosis and apoptosis were determined by western blotting analysis using the following biomarkers or regulatory proteins: CypA, BAX, BAK, Bcl2, and XIAP. Necroptosis was evaluated by measuring the levels of extracellular CypA biomarker protein released from necroptotic cells to an extracellular location. To measure CypA extracellular levels,

80 μl culture media were collected from 10 ml cell culture and mixed with 20 μl 5× SDS-PAGE loading buffer (cat. No. S2002; Biosesang), of which 20 μl was loaded and separated by 12% SDS-PAGE for western blotting. Necroptosis was also analyzed using a Green Fluorescent Protein-Certified Apoptosis/Necrosis Detection kit (cat. No. ENZ-51002; Enzo Life Sciences), according to the manufacturer's protocol. This kit contained 7-aminoactinomycin D (7-AAD) and Annexin V for the detection of necroptosis and apoptosis, respectively. In brief, cells were plated into 8-well chamber slides for 24 h of serum starvation. Cells were observed under confocal microscope (×200) after staining with 7-aminoactinomycin D (7-AAD) to identify necroptotic cells coated in red color and Annexin V-EnzoGold (enhanced Cyanine-3) to detect apoptotic cells stained yellow color.

Transient silencing of XIAP gene and overexpression of TRIP-Br1

For transient knockdown of XIAP, cells were transfected with XIAP silencing siRNA (cat. No. 6446; Cell Signaling Technology) using Turbofect Transfection Reagent (cat. No. R0531) following the manufacturer's instrution. Scrambled RNA (scRNA) was used as a non-silencing control. After 24 h of incubation in DMEM with 10% FBS and 1% antibiotic-antimycotic, the transfection medium was replaced with a fresh medium with or without 10% FBS. For overexpression of TRIP-Br1, SKBr3 cancer cells were transfected with TRIP-Br1 overexpressing pcDNA3.1 plasmid using Turbofect Transfection Reagent (cat. No. R0531) following the manufacturer's instruction, in which pcDNA3.1 plasmid was used as a control vector. After 24 h of incubation in DMEM with 10% FBS and 1% antibiotic-antimycotic, the transfection medium was replaced with a fresh medium with or without 10% FBS and cultured for 24 h and 48 h.

Measurement of mitochondrial membrane potential (MMP)

The MMP was assessed using a Mito-ID Membrane Potential Cytotoxicity kit (cat. No. ENZ-51019; Enzo Life Sciences), according to the manufacturer's protocol. Briefly, MCF-7 cells (~2 × 10^5 cells/well) were seeded into 96-well plates (BD Falcon; BD Biosciences, USA) and cultured in DMEM media with or without 10% FBS for 3, 6, 24, or 48 h. Subsequently, Mito-ID membrane potential dye loading solution was added to each well and incubated at room temperature for 3 h. The MMP was assessed by measuring the resulting fluorescence with a Gemini XPA microplate reader at an excitation wavelength of 480 nm and an emission wavelength of 590 nm.

Measurement of reactive oxygen species (ROS)

Cells were cultured in DMEM media with or without 10% FBS for 24 h and 48 h and then collected into 15 ml conical tubes for centrifugation (Smart R17; Hanil Scientific) at ~200*g* for 2 min. Subsequently, ~5 × 10^4 cells/50 μl PBS were transferred into each well of a 96-well plate and 50 μl of 200 μM 2′,7′-dichlorodihydrofluorescein diacetate (DCFH-DA, cat. No. D399; Thermo Fisher Scientific) was added into each well using a multichannel-pipette (PIPETMAN; Gilson Incorporated, USA) in order to achieve a final concentration of 100 μM DCFH-DA. ROS levels were detected by measuring fluorescence at an excitation wavelength of 485 nm and an emission wavelength of 535 nm every 5 min for 30 min with a Gemini XPA microplate reader.

Preparation of mitochondrial fractions

Cells were then collected into 15 ml conical tubes and centrifuged (Smart R17; Hanil Scientific) at 1,000 rpm for 5 min, washed in ice-cold PBS, and resuspended with hypotonic lysis buffer (220 mM mannitol, 10 mM HEPES, 2.5 mM PO_4H_2K, 1 mM EDTA, 68 mM sucrose, and 1 mM PMSF). They were kept on ice for 60-90 min and then centrifuged at 1,000 rpm for 5 min at 4°C. Cell pellets were resuspended in mitochondrial fraction buffer and pipetted about 10-20 fold gently every 30 min during 1 h incubation on ice. After centrifugation at 1,500-2,000 rpm for 5 min at 4°C and removing cellular debris, the supernatant was transferred to a fresh tube and centrifuged at 10,000-14,000 rpm for 5 min at 4°C. At this stage, the supernatant and pellet represented cytosolic and mitochondrial fractions, respectively. For enhanced purity, the supernatant was centrifuged again following the same protocol. Pellets were resuspended with RIPA buffer and used for western blot analysis as described in Materials and Methods section. Total protein as well as cytosolic and mitochondria fractions were prepared for western blot analysis.

Statistical analysis

Data are presented as mean ± SD from three independent experiments. Statistical analysis was performed using the Student's *t*-test to compare two different groups. The one-way ANOVA followed by Bonferroni's multiple comparisons test, was used to compare multiple groups. SPSS statistics data (ver. 23; IBM, USA) was used for statistical analysis. $P < 0.05$ indicated statistically significant difference.

RESULTS

Necroptosis is induced in various cancer cell lines upon serum starvation, following increased TRIP-Br1 expression

In order to investigate the level of necroptosis in cancer cells upon serum starvation, we first examined the level of necroptosis in various cancer cell lines after culturing them in media with or without serum for 24, 48, or 72 h as mentioned in Materials and Methods section. Necroptosis was evaluated by measuring extracellular levels of CypA, one of the two representative biomarkers of necroptosis (Christofferson and Yuan, 2010). The export of CypA into extracellular media was significantly increased in all the tested cancer cell lines after 72 h, indicating that necroptosis was induced by serum starvation (Figs. 1A and 1B). Interestingly, a relatively very low level of necroptosis was found in MCF-7 cells compared with those in other cancer cell lines. MCF-7 cell line is considered a good study model because of its high degree of resistance to apoptosis underexposure to different stresses or anti-cancer drugs. To find the mechanism how MCF-7 could efficiently suppress necroptosis, we initially focused on TRIP-Br1 oncogenic protein, which was found to be greatly increased in the MCF-7 cell line compared with other cancer cell lines (Figs. 1A and 1B).

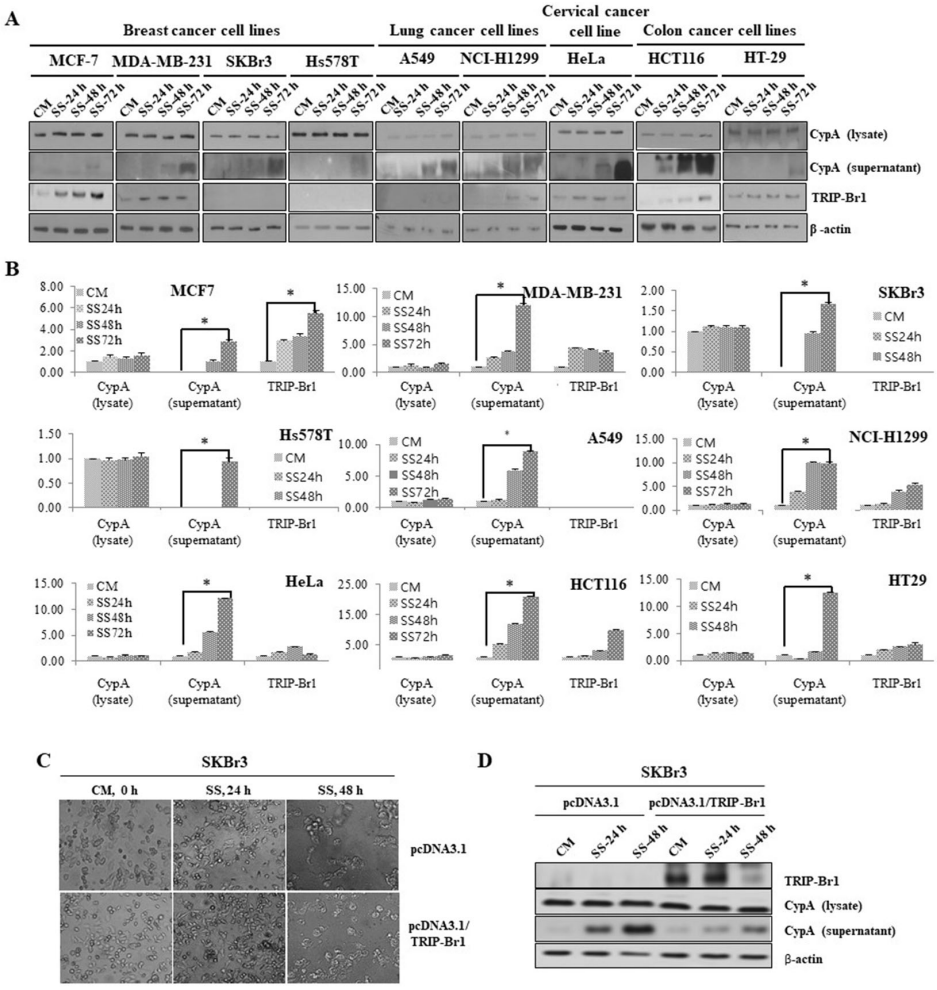

Fig. 1. Levels of necroptosis induction and TRIP-Br1 expression in various cancer cell lines in response to nutrient/serum starved condition. (A) Human breast cancer (MCF-7, MDA-MB-231, SKBr3, and Hs578T), lung cancer (A549 and NCI-H1299), cervical cancer (HeLa), and colon cancer (HCT116 and HT-29) cell lines were cultured in complete media with serum (CM) or serum starved medium (SS) for 24, 48, and 72 h. The level of necroptosis was determined by measuring the extracellular level of CypA (supernatant) as described in Materials and Methods section. TRIP-Br1 expression was also analyzed by western blot analysis, using β-actin as a loading control. All the experiments were performed independently at least triplicate. Representative data are shown. (B) Results of western blot were quantified using ImageJ program. Data are presented as mean ± SD based on three independent experiments. Asterisk (*) indicates statistically significant difference at $P < 0.05$. (C) TRIP-Br1 was overexpressed in SKBr3 breast cancer cells and resulting SKBr3 cells were cultured in complete media with serum (CM) or serum starved medium (SS) for 24 h and 48 h. The morphological changes of SKBr3 cells were photographed under an optical microscope at ×100 magnification. (D) TRIP-Br1 overexpressing SKBr3 cells were subjected to western blot analysis to determine the levels of necroptosis by measuring the extracellular level of CypA (supernatant), in which β-actin as a loading control.

The relatively very low level of necroptosis was induced in MCF-7 cancer cell line, following increased expression of TRIP-Br1 protein implies that TRIP-Br1 might be responsible for the inhibition of necroptosis in response to serum starvation. Therefore, the effect of TRIP-Br1 on necroptosis was further investigated in SKBr3 breast cancer cell line because this cell line shows high level of necroptosis under serum starvation and no TRIP-Br1 expression (Figs. 1A and 1B). Our result showed that necroptosis was significantly repressed in TRIP-Br1 overexpressing SKBr3 cancer cells compared with control cells, implying that TRIP-Br1 can suppress necroptosis under serum starved condition (Figs. 1C and 1D).

Taken together, our data imply that TRIP-Br1 may play an important role in necroptosis. Therefore, the role of TRIP-Br1 in necroptosis was further investigated in MCF-7 cells under serum starvation.

Necroptosis is accelerated in TRIP-Br1 knock-downed MCF-7 cancer cells in response to nutrient depletion

Based on the inhibitory role of TRIP-Br1 in apoptosis and the inverse relationship between the degree of necroptosis induction and TRIP-Br1 expression, we hypothesized that elevated TRIP-Br1 expression suppressed serum starvation-induced necroptosis. To test this hypothesis, MCF-7 stable cell

lines carrying wild-type TRIP-Br1 gene (MCF-7$^{WT\text{-}TRIP\text{-}Br1}$) or knock-downed TRIP-Br1 gene (MCF-7$^{KD\text{-}TRIP\text{-}Br1}$) were cultured in serum containing the complete medium (CM) or serum starved medium (SS) for 24, 48, and 72 h. Microscopic images revealed that MCF-7$^{KD\text{-}TRIP\text{-}Br1}$ cells showed significantly slower proliferation and a dramatic increase in cell death after 72 h of serum starvation compared with MCF-7$^{WT\text{-}TRIP\text{-}Br1}$ cells (Fig. 2A). Our western blot analysis showed that the extracellular level of CypA was substantially elevated in MCF-7$^{KD\text{-}TRIP\text{-}Br1}$ cells than in MCF-7$^{WT\text{-}TRIP\text{-}Br1}$ cells after 72 h of serum starvation, indicating that the elevated TRIP-Br1 suppressed necroptosis in MCF-7 cells under serum starvation (Figs. 2B

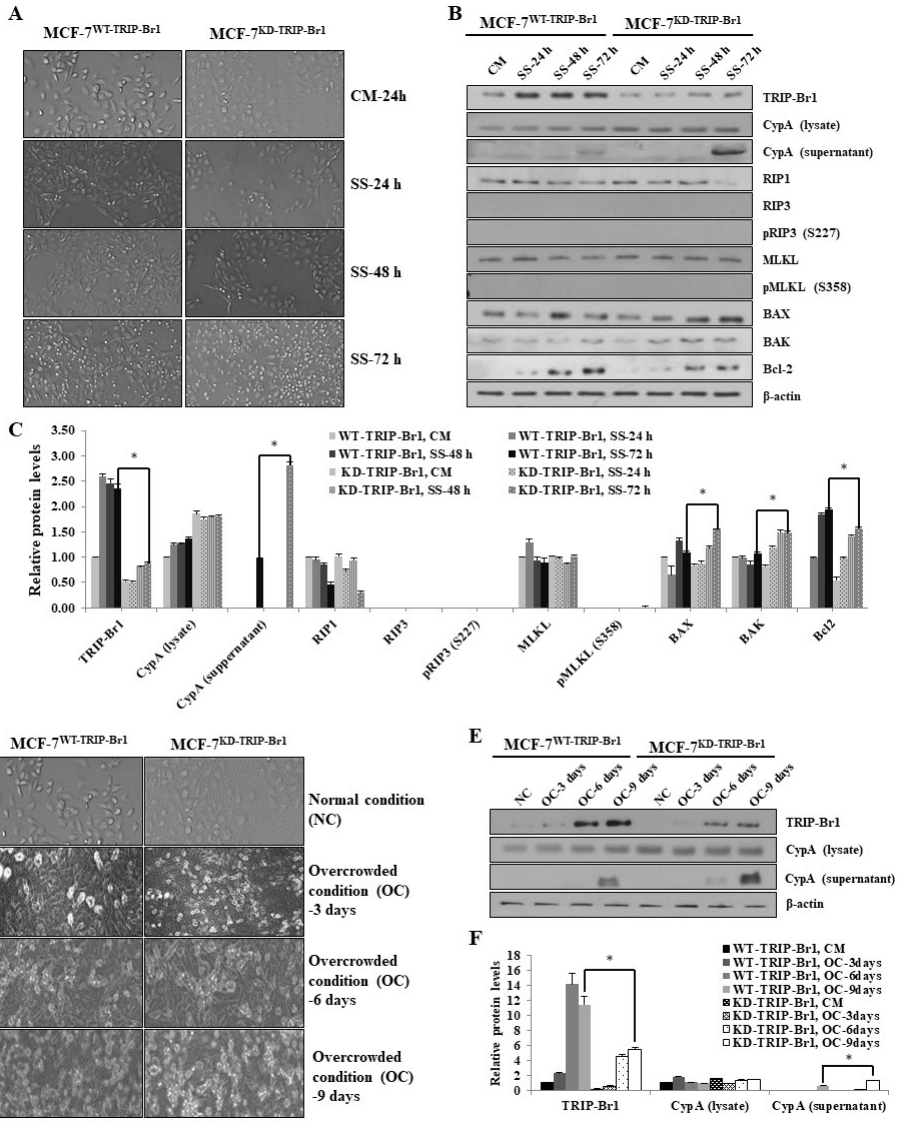

Fig. 2. Inhibitory role of TRIP-Br1 in necroptosis under nutrient depleted conditions, serum starvation, or overcrowded environment. (A) Stable MCF-7$^{WT\text{-}TRIP\text{-}Br1}$ and MCF-7$^{KD\text{-}TRIP\text{-}Br1}$ cell lines were seeded at a density of ~1 × 10^6 cells into 10-cm dishes and cultured either in complete media (CM) or serum starved media (SS) for 24, 48, and 72 h. The morphological changes were photographed under an optical microscope at ×100 magnification. (B) Cells were collected and subjected to western blot analysis to determine the levels of necroptosis and related protein expression, using β-actin as a loading control. All the experiments were performed independently at least in triplicate. Representative data are shown. (C) Results of western blot were quantified using ImageJ program. Data are presented as mean ± SD based on three independent experiments. $*P < 0.05$. (D) MCF-7$^{WT\text{-}TRIP\text{-}Br1}$ and MCF-7$^{KD\text{-}TRIP\text{-}Br1}$ stable cell lines were seeded at a density of ~10^6 cells/100-mm plate and grown in normal condition (NC) with complete cell culture media until they reach approximately 50% confluence or in overcrowded conditions (OC) with high levels of cell confluence by culturing for 3, 6, and 9 days. The morphological images were analyzed under an optical microscope at 100× magnification. (E) After the lapse of the indicated time period, cells were collected and subjected to western blot analysis to determine the effect of TRIP-Br1 on necroptosis by measuring the extracellular levels of CypA as a biomarker, β-actin as a loading control. All experiments were performed independently at least in triplicate. Representative data are shown. (F) Western blot results were quantified using ImageJ program. Data are presented as mean ± SD based on three independent experiments. $*P < 0.05$.

and 2C). We also analyzed the effect of TRIP-Br1 on vital regulators in necroptosis, including RIP1, RIP3, and MLKL using western blot analysis. Our data showed that RIP1 level was significantly decreased in MCF-7$^{KD\text{-}TRIP\text{-}Br1}$ cells than in MCF-7$^{WT\text{-}TRIP\text{-}Br1}$ cells after 72 h of serum starvation (Figs. 2B and 2C). Our data also revealed the lack of RIP3 expression, and therefore the absence of RIP3 phosphorylation in MCF-7$^{WT\text{-}TRIP\text{-}Br1}$ and MCF-7$^{KD\text{-}TRIP\text{-}Br1}$ cells (Fig. 2B). These results are consistent with previous studies, which reported that the MCF-7 cell line lacks RIP3 (He et al., 2009). Furthermore, it is also known that phosphorylated RIP3 activates MLKL via phosphorylation. Accordingly, we determined the effect of TIRP-Br1 on MLKL phosphorylation. Our data revealed a lack of MLKL phosphorylation despite the presence of MLKL (Fig. 2B). This result suggested the presence of another pathway inducing the necroptosis in the absence of RIP3 or MLKL activation. Next, we analyzed the representative pro-apoptotic proteins of BAX and BAK and anti-apoptotic protein Bcl2, which are known to mediate many other types of cell deaths including necroptosis (Karch et al., 2013; 2015; Lindqvist et al., 2014; Nikoletopoulou et al., 2013). The expression of BAX and BAK was found to be slightly higher in MCF-7$^{KD\text{-}TRIP\text{-}Br1}$ cells than in MCF-7$^{WT\text{-}TRIP\text{-}Br1}$ cells (Figs. 2B and 2C). By contrast, the Bcl2 expression was significantly lower in MCF-7$^{KD\text{-}TRIP\text{-}Br1}$ cells than in MCF-7$^{WT\text{-}TRIP\text{-}Br1}$ cells (Figs. 2B and 2C). These data suggest that TRIP-Br1suppressed necroptosis at least partly by regulating expression of BAX, BAK, and Bcl2 (Figs. 2B and 2C).

In an extended study, we also analyzed the effect of TRIP-Br1 on necroptosis under overcrowded stress, a type of nutrient depletion mostly occurring *in vivo*. Microscopic images showed a lower growth but higher death of MCF-7$^{KD\text{-}TRIP\text{-}Br1}$ cells than in MCF-7$^{WT\text{-}TRIP\text{-}Br1}$ cells (Fig. 2D). Consistent with serum starvation results, the extracellular CypA level was significantly higher in MCF-7$^{KD\text{-}TRIP\text{-}Br1}$ cells than in MCF-7$^{WT\text{-}TRIP\text{-}Br1}$ cells after 9 days of culture. The CypA exportation in MCF-7$^{KD\text{-}TRIP\text{-}Br1}$ cells started on day 6 of overcrowded culture and was greatly elevated on day 9 of culture (Figs. 2E and 2F).

These results suggest that the presence of TRIP-Br1 in MCF-7 cells apparently suppressed the necroptosis under nutrient deprivation such as serum starvation or overcrowded conditions.

TRIP-Br1 inhibits necroptosis by repressing ROS generation and suppressing CypD release from mitochondria into cytosol

To determine the inhibitory role of TRIP-Br1 in necroptosis, we hypothesized that TRIP-Br1 suppressed necroptosis by interfering with PCD-related mitochondrial functions, including the maintenance of MMP or the production of ROS. Our previous study showed the presence of a great amount of TRIP-Br1 in the mitochondria (Jung et al., 2015). The cellular role of mitochondria attracted significant attention in apoptosis over the years. Recent studies have demonstrated the role of mitochondria in different types of cell death including necroptosis, in which necroptosis as well as apoptosis were characterized by decreased MMP and increased ROS production (Bernardi et al., 2006; Dashzeveg and Yoshida, 2015; Geou-Yarh Liou, 2010; Karch et al., 2015; Lin et al., 2004; Marchi et al., 2012; Montero et al., 2013; Redza-Dutordoir and Averill-Bates, 2016; Rohde et al., 2017; Tsujimoto and Shimizu, 2007; Vaseva et al., 2012). Nutrient starvation induces ROS increase, plasma membrane permeabilization, and eventually necroptosis. Therefore, we hypothesized that TRIP-Br1 might inhibit necroptosis by preventing the loss of MMP and the generation of ROS. Accordingly, the cellular levels of MMP and ROS were estimated in MCF-7$^{WT\text{-}TRIP\text{-}Br1}$ and MCF-7$^{KD\text{-}TRIP\text{-}Br1}$ cell lines under serum starvation.

First, the effect of TRIP-Br1 on MMP was analyzed after MCF-7$^{WT\text{-}TRIP\text{-}Br1}$ and MCF-7$^{KD\text{-}TRIP\text{-}Br1}$ cells. The MMP level was significantly decreased after 3 h of serum starvation in both cell lines (Figs. 3A and 3B). However, no significant differences in MMP level were detected between MCF-7$^{WT\text{-}TRIP\text{-}Br1}$ and MCF-7$^{KD\text{-}TRIP\text{-}Br1}$ cells, indicating that TRIP-Br1 protein did not affect the MMP level under serum starvation.

Second, the effect of TRIP-Br1 on cellular ROS generation was also analyzed in MCF-7$^{WT\text{-}TRIP\text{-}Br1}$ and MCF-7$^{KD\text{-}TRIP\text{-}Br1}$ cells. A gradual increase in ROS level was observed on both cell lines after 24 h of serum starvation (Fig. 3C). Interestingly, the ROS accumulation was significantly higher in MCF-7$^{KD\text{-}TRIP\text{-}Br1}$ cells after 48 h of serum starvation than in MCF-7$^{WT\text{-}TRIP\text{-}Br1}$ cells (Fig. 3C). These data indicate that TRIP-Br1 suppressed ROS production in response to serum starvation. In a further study, we analyzed the mitochondrial proteins that play an important role in necroptosis and apoptosis. Mitochondria induce necroptosis and apoptosis by releasing pro-necroptotic or pro-apoptotic proteins, respectively. Mitochondrial permeability transition pore (MPTP) opening as an inner mitochondrial membrane event results in mitochondrial swelling, and necrotic cell death whereas mitochondrial outer membrane permeabilization (MOMP) predominantly leads to apoptosis (Karch et al., 2013). During necroptosis, the increased ROS induces the opening of MPTP in the mitochondrial matrix. This pore opening event leads to mitochondrial depolarization and eventually leads to organelle rupture (Halestrap, 2009). Although the actual pore forming component of MPTP remains unclear, cyclophilin D (CypD) is known as a vital regulator of MPTP opening and necrotic cell death. It is localized in the mitochondrial matrix and released into the cytosol upon exposure to necroptosis inducing stress. Therefore, we determined the CypD level in mitochondria and cytosol following mitochondrial fractionation as described in Materials and Methods section. Our western blot data revealed that the TRIP-Br1 protein expression was highly increased in mitochondria in response to serum starvation (Figs. 3D and 3E). Interestingly, the release of CypD from mitochondria to cytosol was significantly lower in MCF-7$^{WT\text{-}TRIP\text{-}Br1}$ cells than in MCF-7$^{KD\text{-}TRIP\text{-}Br1}$ cells after 72 h of serum starvation, indicating that TRIP-Br1 inhibited the release of CypD into cytosol under serum starvation (Figs. 3D and 3E). Our data also showed that Cyt C release, a characteristic of apoptosis, was slightly higher in MCF-7$^{KD\text{-}TRIP\text{-}Br1}$ cells than in MCF-7$^{WT\text{-}TRIP\text{-}Br1}$ cells (Figs. 3D and 3E), although the difference between the two was not statistically significant. This finding suggests that elevated TRIP-Br1 in mitochondria predominantly inhibited necroptosis by negatively affecting the release of CypD from the mitochondrial matrix into the cytosol rather than apoptosis. Another important mitochondrial division related protein Drp1 did not show any significant difference between MCF-7$^{WT\text{-}}$

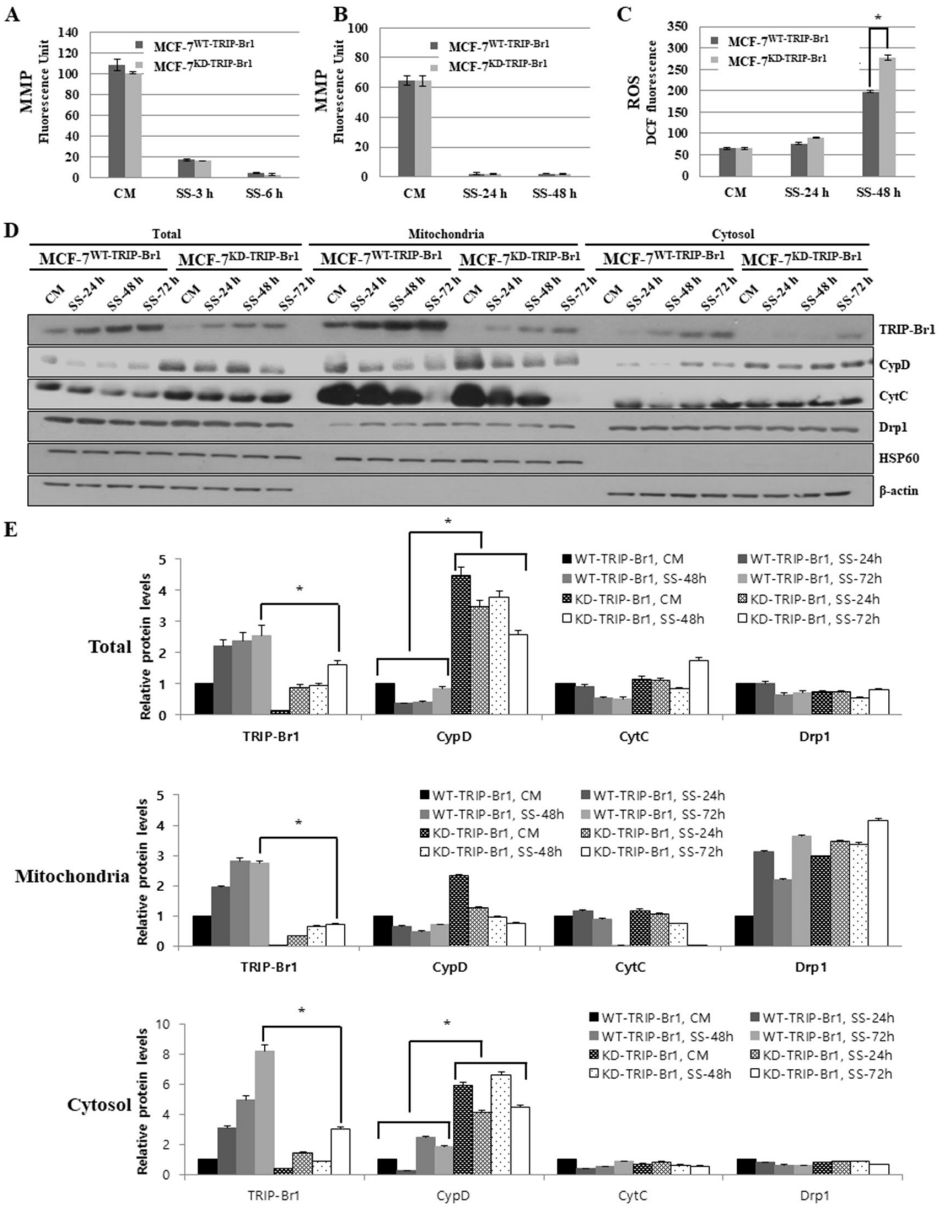

Fig. 3. Effect of TRIP-Br1 on mitochondrial functions (MMP and ROS generation) and the release of necroptosis inducer (CypD) in response to serum starvation. Stable MCF-7$^{WT\text{-}TRIP\text{-}Br1}$ and MCF-7$^{KD\text{-}TRIP\text{-}Br1}$ cell lines were incubated in media with or without serum for the indicated durations. (A and B) MMP was tested as described in Materials and Methods section after MCF-7$^{WT\text{-}TRIP\text{-}Br1}$ and MCF-7$^{KD\text{-}TRIP\text{-}Br1}$ cells were cultured in complete media (CM) or serum starved (SS) media under two different conditions: short (3 h and 6 h), and long (24 h and 48 h) exposure to serum starvation. Data are presented as mean ± SD based on three independent experiments. $*P < 0.05$. (C) Cellular ROS levels were measured as described in Materials and Methods section after culturing MCF-7$^{WT\text{-}TRIP\text{-}Br1}$ and MCF-7$^{KD\text{-}TRIP\text{-}Br1}$ cells in complete media (CM) and serum starved (SS) media for 24 h and 48 h. Intracellular ROS levels were evaluated using 2', 7'-dichlorodihydrofluorescein. Data are presented as mean ± SD based on three independent experiments. $*P < 0.05$. DCF, dichlorofluorescein. (D) Stable MCF-7$^{WT\text{-}TRIP\text{-}Br1}$ and MCF-7$^{KD\text{-}TRIP\text{-}Br1}$ cell lines were cultured in either complete media (CM) or serum starved medium (SS) for 24, 48, and 72 h followed by mitochondrial fractionation as described in Materials and Methods section. Isolated protein fractions were analyzed using western blot for protein expression. HSP60 was used as a mitochondrial marker and β-actin as a cytosolic fractionation marker. (E) Results of western blot were quantified using ImageJ program. Data are presented as mean ± SD based on three independent experiments. $*P < 0.05$.

$^{TRIP\text{-}Br1}$ and MCF-7$^{KD\text{-}TRIP\text{-}Br1}$ cells in response to serum starvation, suggesting that TRIP-Br1 had no effect on Drp1 (Figs. 3D and 3E). Our mitochondrial fractionation data also showed that TRIP-Br1 protein expression was significantly increased in mitochondria after a relatively short exposure (3 h) to serum starvation, although no significant changes in total TRIP-Br1

protein level were observed (data not shown). This finding indicates mitochondrial translocation of TRIP-Br1 from the cytosol immediately after exposure to serum starvation.

Taken together, our data indicate that up-regulated TRIP-Br1 inhibited necroptosis at least partly by repressing mitochondrial ROS production and interfering with the release of CypD from mitochondria into cytosol in MCF-7 cells under serum starvation.

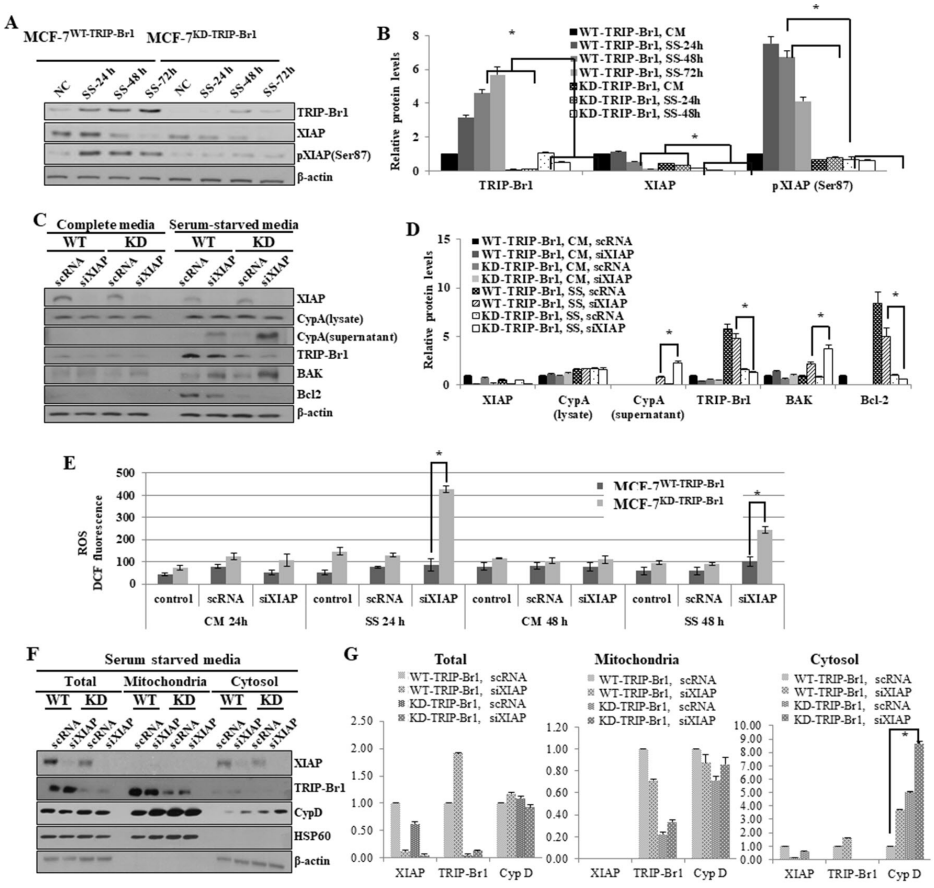

Fig. 4. Enhanced inhibition of TRIP-Br1-mediated necroptosis by XIAP via repression of ROS production and suppression of CypD exportation. (A) Stable MCF-7$^{WT\text{-}TRIP\text{-}Br1}$ and MCF-7$^{KD\text{-}TRIP\text{-}Br1}$ cells were cultured in either complete media (CM) or serum starved medium (SS) for 24 h or 48 h. Resulting cells were collected and western blot was performed as described in Materials and Methods section. All experiments were performed independently at least in triplicate. Representative data are shown. (B) Western blot results were quantified using ImageJ program. Data are presented as mean ± SD based on three independent experiments. $*P < 0.05$. (C) Stable MCF-7$^{WT\text{-}TRIP\text{-}Br1}$ and MCF-7$^{KD\text{-}TRIP\text{-}Br1}$ cells (1×10^6) were seeded into 10-cm dishes. These cells were transiently transfected with XIAP silencing siRNA (siXIAP), in which scrambled RNA (scRNA) was used as a non-silencing control. Cells were incubated in media with or without serum for 48 h. Cell extracts were analyzed using western blot β-actin as a loading control. All experiments were performed independently at least in triplicate. Representative data are shown. WT, MCF-7$^{WT\text{-}TRIP\text{-}Br1}$; KD, MCF-7$^{KD\text{-}TRIP\text{-}Br1}$. (D) Results of western blot were quantified by using ImageJ program. Data are presented as mean ± SD based on three independent experiments. $*P < 0.05$. (E) Inhibitory effect of TRIP-Br1/XIAP on ROS generation in MCF-7 cells in response to serum starvation. Stable MCF-7$^{WT\text{-}TRIP\text{-}Br1}$ and MCF-7$^{KD\text{-}TRIP\text{-}Br1}$ cell lines were cultured in complete media (CM) or serum-starved media (SS) for 24 h or 48 h. Cells were transiently transfected with XIAP silencing siRNA (siXIAP), using scrambled RNA (scRNA) as a non-silencing control. Cells were then incubated in media with or without serum for 48 h and the cellular ROS level was measured as described in Materials and Methods section. After cells were transiently transfected with siXIAP, using scRNA as a non-silencing control, cells were incubated in media with or without serum for 24 h and 48 h. The cells were collected and 2.5×10^4 cells were cultured in 96-well tissue culture dishes, ROS levels were measured after adding DCFH-DA. All experiments were performed independently at least three times. Representative data are shown. Western blot results were quantified by using ImageJ program. Data are presented as mean ± SD based on three independent experiments. $*P < 0.05$. (F) MCF-7$^{WT\text{-}TRIP\text{-}Br1}$ (WT) and MCF-7$^{KD\text{-}TRIP\text{-}Br1}$ cells (KD) (2.5×10^4) were seeded into 10-cm dishes. After synchronization, cells were transiently transfected with siXIAP, using scRNA as a non-silencing control. Cells were then incubated in media with or without serum for 24 h, followed by mitochondrial fractionation. Isolated protein fractions were analyzed with western blot for the determination of protein expression. HSP60 was used as a mitochondrial marker and β-actin was used as a cytosolic fractionation marker. (G) Western blot results were quantified by using ImageJ program. Data are presented as mean ± SD based on three independent experiments. $*P < 0.05$.

XIAP enhances the inhibitory effect of TRIP-Br1 on necroptosis under serum starvation

During the elucidation of the molecular mechanism underlying the inhibitory effect of TRIP-Br1 on necroptosis, we hypothesized that TRIP-Br1 worked with XIAP in necroptosis inhibition under serum starvation. Our previous study showed that TRIP-Br1 directly bound XIAP and stabilized, and eventually inhibited apoptosis (Hong et al., 2009). It is known that XIAP is activated by phosphorylation at the Ser87 residue and the activated XIAP inhibits apoptosis (Kato et al., 2011). Thus, we first determined the XIAP expression and phosphorylation levels after the MCF-7$^{WT\text{-}TRIP\text{-}Br1}$ and MCF-7$^{KD\text{-}TRIP\text{-}Br1}$ cells were cultured in complete or serum-starved media for 24, 48, and 72 h. Our data revealed that the XIAP levels were decreased in both cell lines in a time-dependent manner (Figs. 4A and 4B). However, the XIAP level substantially higher in MCF-7$^{WT\text{-}TRIP\text{-}Br1}$ than in MCF-7$^{KD\text{-}TRIP\text{-}Br1}$ cells (Figs. 4A and 4B). In addition, phosphorylation of XIAP at Ser87 residue was strongly increased in MCF-7$^{WT\text{-}TRIP\text{-}Br1}$ cells, but not in MCF-7$^{KD\text{-}TRIP\text{-}Br1}$ cells (Figs. 4A and 4B). These data suggest that TRIP-Br1 boosted XIAP activation via phosphorylation as well as stabilized XIAP protein expression.

To elucidate the XIAP-dependent TRIP-Br1 inhibition in necroptosis, siXIAP was introduced into MCF-7$^{WT\text{-}TRIP\text{-}Br1}$ and MCF-7$^{KD\text{-}TRIP\text{-}Br1}$ cells to silence XIAP. Our results showed that the double knock-down of TRIP-Br1 and XIAP greatly enhanced necroptosis. We showed that CypA exportation was significantly increased in TRIP-Br1 single knock-downed cell (MCF-7$^{KD\text{-}TRIP\text{-}Br1}$) after 72 h of serum starvation (Fig. 2B). However, the double knock-down of TRIP-Br1 and XIAP resulted in a dramatic increase of extracellular CypA level after 24 h of serum starvation (Figs. 4C and 4D). This result strongly suggests that inhibition of necroptosis by TRIP-Br1 greatly enhanced by XIAP in conjunction with TRIP-Br1. The current study also showed that XIAP silencing marginally reduced TRIP-Br1 protein expression suggesting that XIAP also positively affected the stability of TRIP-Br1 (Figs. 4C and 4D).

To determine how XIAP enhanced the inhibitory role of TRIP-Br1 in serum starvation–induced necroptosis, we hypothesized that TRIP-Br1/XIAP suppressed necroptosis by regulating mitochondrial proteins involved in different types of cell death including necroptosis. Necroptosis-inducing stimuli increase both BAX/BAK pro-apoptotic proteins to generate MPTP openings as well as apoptotic pores in the outer mitochondrial membrane while Bcl2 negatively affects this process (Karch et al., 2015). We therefore analyzed these proteins in both MCF-7$^{WT\text{-}TRIP\text{-}Br1}$ and MCF-7$^{KD\text{-}TRIP\text{-}Br1}$ cells transfected with either scRNA or siXIAP. Our data revealed significantly higher levels of BAK but substantially lower levels of Bcl2 in XIAP silenced MCF-7$^{KD\text{-}TRIP\text{-}Br1}$ cells compared with MCF-7$^{WT\text{-}TRIP\text{-}Br1}$ cells, suggesting that XIAP exhibited negative against BAK and but positive effects on Bcl2 under serum starvation which might possibly trigger higher levels of necroptosis (Figs. 4C and 4D).

It is also well known that Bcl2 strongly affects the intracellular ROS level (Aharoni-Simon et al., 2016). Thus, the effect of TRIP-Br1/XIAP on cellular ROS level was assessed. The ROS level greatly increased in MCF-7$^{KD\text{-}TRIP\text{-}Br1}$ at 24 h after treatment with siXIAP whereas it was slightly increased in MCF-7$^{WT\text{-}TRIP\text{-}Br1}$ treated with siXIAP (Fig. 4E). However, ROS level was decreased ~50% after 48 h of treatment probably due to cell death (Fig. 4E). These data strongly suggest that necroptosis suppression by TRIP-Br1 via repression of ROS levels is greatly enhanced by XIAP under serum starvation.

We showed that up-regulated TRIP-Br1 inhibited the release of CypD into cytosol and and abrogated necroptosis. Subsequently, the CypD levels in mitochondria and cytosol were also evaluated after silencing XIAP in MCF-7$^{WT\text{-}TRIP\text{-}Br1}$ and MCF-7$^{KD\text{-}TRIP\text{-}Br1}$ cells (Figs. 4F and 4G). Our western blot analysis showed that release of CypD protein was significantly increased in the cytosol of MCF-7$^{KD\text{-}TRIP\text{-}Br1}$ cells with following XIAP gene silencing compared with that the expression in the cytosol of MCF-7$^{WT\text{-}TRIP\text{-}Br1}$ cells with silenced XIAP (Figs. 4F and 4G). This result suggests that XIAP enhanced the inhibitory effect of TRIP-Br1 on necroptosis by interfering with the release of CypD into cytosol.

The induction of both necroptosis and apoptosis was determined by confocal microscopy, in which 7-AAD and Annexin V staining were used to detect necroptosis and apoptosis, respectively (Fig. 5). Both cell lines showed strong fluorescence signals of 7-AAD and slight staining of Annexin V, indicating predominant induction of necroptosis rather than apoptosis in MCF-7 cells (Fig. 5). Taken together, our data indicate that XIAP enhanced the inhibitory effect of TRIP-Br1 on necroptosis under serum starvation. In addition, TRIP-Br1/XIAP suppressed necroptosis at least partly by suppressing cellular ROS levels and the release of CypD into cytosol under serum starvation.

TRIP-Br1 inhibits shikonin-mediated necroptosis but not TNF-α-mediated necroptosis

In an extended study, we tested whether TRIP-Br1 also suppressed necroptosis in response to other types of necroptosis inducers such as TNF-α and shikonin. Currently, TNF-α combined with caspase inhibitors and IAP inhibitors is widely used as classical necroptosis inducer (Cai et al., 2014; He et al., 2009; Moriwaki et al., 2015; Wang et al., 2014). Similar to results under serum starvation, TRIP-Br1 was also elevated in MCF-7 cells but not in HT-29 colon cancer cells. The HT-29 cell line was used as a control because this cell line has complete necroptotic machinery including RIP3 and MLKL. The XIAP level was found to be stable in MCF-7$^{WT\text{-}TRIP\text{-}Br1}$ cells. The combined treatment of TNF-α, zVAD-fmk, and Smac mimetic efficiently induced necroptosis of HT-29 colon cancer cells whereas no sign of necroptosis was detected in MCF-7 cells when cells were subjected to the same treatment (Figs. 6A and 6B). These results are consistent with other studies, suggesting that MCF-7 is strongly resistant to TNF-α treatment. In HT-29 cells, the RIP3 expression level was increased after TNF-α treatment and accordingly, the phosphorylation of MLKL was also increased (Figs. 6A and 6B). However, no RIP3 or no MLKL phosphorylation was detected in MCF-7 cells (Figs. 6A and 6B). These data also suggest that TNF-α-mediated necroptosis requires necroptotic mediators such as RIP3 and MLKL.

Next, we used another necroptosis-inducing agent shikonin to treat MCF-7 cells. He et al. (2009) have suggested that the combined treatment of TNF-α, zVAD-fmk, and Smac mimetic agents is not effective against MCF-7 cells. However,

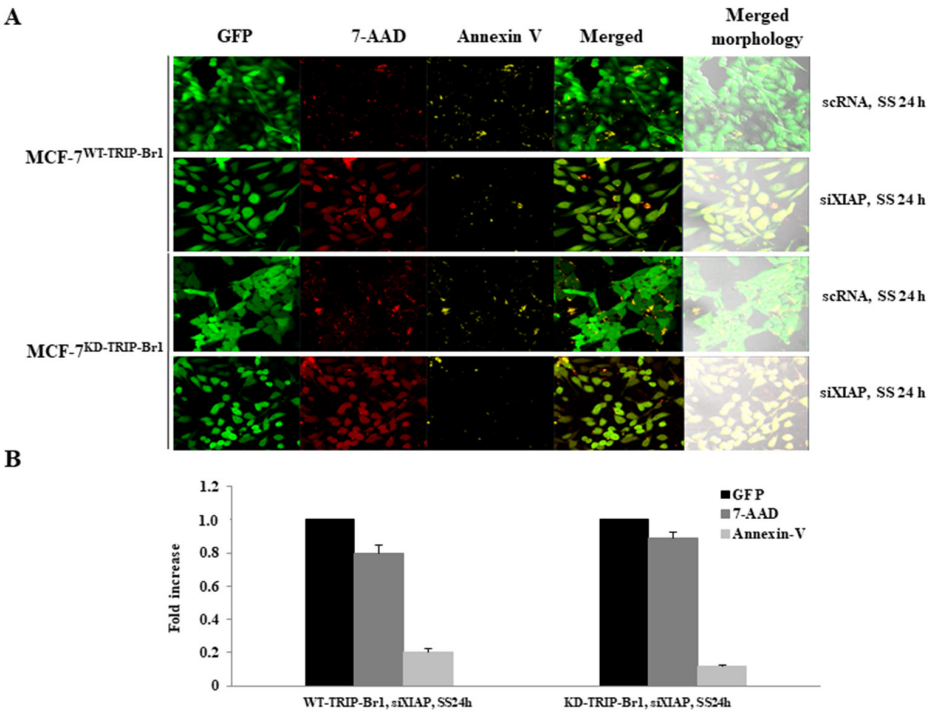

Fig. 5. Negative effect of TRIP-Br1/XIAP on necroptosis and apoptosis. (A) Cells (2×10^5) were cultured in complete media for 24 h after seeding 2×10^5 cells into a 35-mm confocal dish. Resulting cells were transiently transfected with siXIAP, using scRNA as a non-silencing control and incubated in media without serum (SS) for 24 h. Cells were observed under confocal microscope (magnification, ×200) after staining with Annexin V-EnzoGold (enhanced Cyanine-3) to detect apoptotic cells labeled yellow and necroptotic cells stained with 7-Aminoactinomycin D (7-AAD) were detectedin red as described in Materials and Methods section. (B) Results were semi-quantified using ImageJ. Data are presented as mean ± SD based on three independent experiments.

Han et al. (2007) have proposed that a naturally occurring compound such as shikonin induces necroptosis in MCF-7 cells despite the lack of RIP3. Therefore, we analyzed the effect of TRIP-Br1 on shikonin-mediated necroptosis in MCF-7 cells. Exportation of CypA occurred in both MCF-$7^{WT\text{-}TRIP\text{-}Br1}$ and MCF-$7^{KD\text{-}TRIP\text{-}Br1}$ cell lines after treatment with 50 or 100 μM of shikonin, in which a relatively higher level of CypA exportation was detected in MCF-$7^{KD\text{-}TRIP\text{-}Br1}$ cells (Figs. 6C and 6D). These data indicate that shikonin induced necroptosis of MCF-7 cells, and MCF-$7^{KD\text{-}TRIP\text{-}Br1}$ cells were strongly sensitive to shikonin compared with MCF-$7^{WT\text{-}TRIP\text{-}Br1}$ cells. These data strongly suggest that MCF-7 cells are highly resistant to TNF-α, but sensitive to shikonin. In addition, TRIP-Br1 repressed serum-starved or shikonin-induced necroptosis, but not TNF-α-mediated necroptosis, strongly suggesting the presence of another pathway for necroptosis in response to different types of stress or stimuli.

DISCUSSION

A major challenge in cancer treatment involves the resistance of cancer cells to cell death, especially apoptosis. Therefore, we tried to trigger necroptosis as an alternative to cell death besides apoptosis. Understanding the necroptotic mechanism, especially the similarities and differences between apoptosis and necroptosis, may provide valuable insights into the design and development of effective cancer therapies. In this study, we described a novel inhibitory role of TRIP-Br1/XIAP in necroptosis under nutrient/serum starvation.

Other research groups in addition to our data showed that MCF-7 cells were highly resistant to necroptosis and apoptosis in response to necroptosis-inducing stresses, possibly due to the absence of a key protein in necroptotic machinery (e.g., RIP3 for necroptosis). The RIP1-RIP3-MLKL machinery, a core signaling pathway in necroptosis, is considered an important tumor suppression mechanism and inhibitor of cancer progression (Cai et al., 2014; He et al., 2009; Moriwaki et al., 2015; Wang et al., 2014). Thus, cancer cells appear to enhance tumorigenesis by suppressing necroptosis via down-regulation or induction of functional mutations in RIP3 and MLKL genes. Moriwaki et al. (2015) have proposed that RIP1 expression level is decreased only in a few cancer cells whereas RIP3 expression is down-regulated in numerous cancer cells. For example, HeLa cervical cancer cells are well-known for their resistance to necroptosis. They express normal levels of RIP1 without expressing RIP3 (Su et al., 2016; Wang et al., 2012). Other research groups in addition to our data also showed the lack of MLKL phosphorylation probably due to the absence of RIP3 in MCF-7 cells. However, our data also showed that necroptosis was induced in MCF-7 cells in response to serum starvation. Therefore, elucidation of the mechanism of necroptosis in these cancer cells without acti-

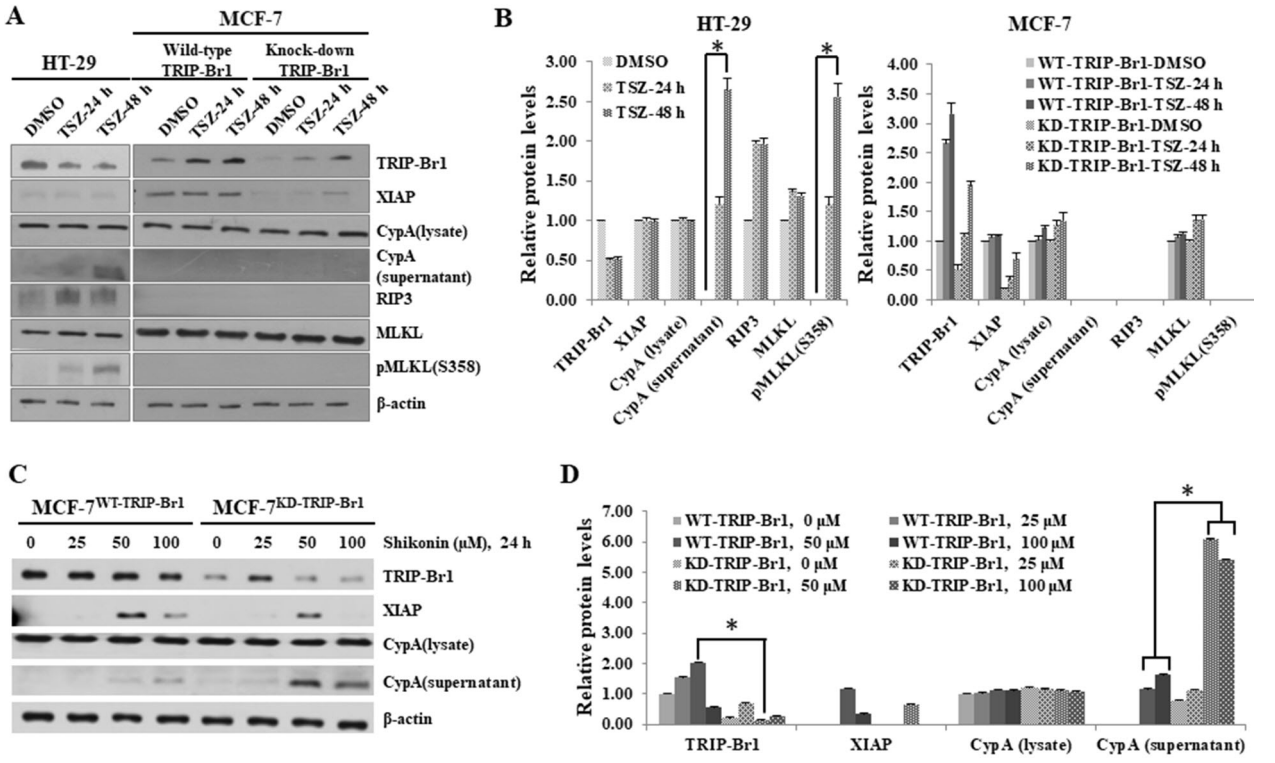

Fig. 6. Effect of TRIP-Br1 on necroptosis of MCF-7 cells in response to other necroptosis inducing agents (TNF-α and shikonin). (A) To induce necroptosis without apoptosis, HT-29 and MCF-7 cells (1×10^6) were grown in complete growth media, followed by treatment with 100 ng/ml TNF-α for 24 h and 48 h along with 20 μM zVAD-fmk and 100 μM of Smac mimetic as caspase inhibitor and IAP antagonizer, respectively. HT-29 colon cancer cells served as control to determine the efficiency of necroptosis induction. After the indicated time periods, cells were collected and subjected to western blot. All experiments were performed independently at least in triplicate. Representative data are shown. (B) Western blot results were quantified using ImageJ program. Data are presented as mean ± SD based on three independent experiments. $*P < 0.05$. (C) MCF-7 cells (1×10^6) were treated with shikonin, a specific necroptosis inducer of MCF-7 cells, at different concentrations (0, 25, 50, and 100 μM) of shikonin for 24 h. Cells were collected and subjected to western blot analysis. (D) Western blot results were quantified by using ImageJ program. Data are presented as mean ± SD based on three independent experiments. $*P < 0.05$.

vation of RIP3 or MLKL as key components is of great interest. Our data showed that MCF-7 cell line exhibited robust resistance to necroptosis in response to TNF-α treatment, which might be associated with altered subcellular localization of p21CIP1 and p27KIP1 (Wang et al., 2005). Cells lacking RIP3 use different pathways and regulators for necroptosis. A key factor may be cellular ROS level. He et al. (2009) have suggested that ROS scavengers have no effect on TNF-α with zVAD-fmk and Smac mimetic induced necroptosis in HT-29, suggesting that ROS are not involved in necroptosis of HT-29 (He et al., 2009; Marshall and Baines, 2014). However, our study showed that ROS was highly involved in serum starvation-induced necroptosis in MCF-7 cells, in which TRIP-Br1/XIAP inhibited necroptosis by suppressing cellular ROS level.

Our previous and current data showed that TRIP-Br1/XIAP inhibited both necroptosis and apoptosis (Jung et al., 2015), and possibly regulated RIP1 stability. RIP1 is initially polyubiquitinylated with Lys63-linked chains by cIAP E3 ligase within the complex I after recruitment to the membrane. The modified RIP1 serves as a signaling platform for the activation of nuclear factor-kappaB (NFκB) and inhibits caspase8 cleavage, eventually resulting in cell survival instead of inducing apoptosis or necroptosis (Newton and Manning, 2016). XIAP is an E3 ligase belonging to the IAP family and is necessary for ubiquitination. Therefore, TRIP-Br1/XIAP inhibit apoptosis and necroptosis by regulating RIP1 ubiquitination.

Our previous data showed that TRIP-Br1 stabilized XIAP and inhibited apoposis (Hong et al., 2009). The current study also showed that TRIP-Br1 level was significantly reduced when XIAP was silenced in cells (Fig. 4C). Thus, XIAP enhance TRIP-Br1 stability directly or indirectly, via unknown mechanism. A previous study showed that PKC phosphorylated XIAP at Ser87 residues and PKB was associated with cell survival and protection againt apoptosis (Dan et al., 2004; Kato et al., 2011). Interestingly, our data showed that XIAP phosphorylation was higher in MCF-$7^{WT\text{-}TRIP\text{-}Br1}$ cells than in MCF-$7^{KD\text{-}TRIP\text{-}Br1}$ cells under serum starvation. Therefore, TRIP-Br1 may positively regulate XIAP phosphorylation at Ser87 by modulating PKC and AKT espression. The precise mechanism underlying the effect of TRIP-Br1 and pXIAP remains unclear, underscoring the need for further investigation.

Various types of cell death include apoptosis, caspase-independent apoptosis, autophagy-mediated cell death, necroptosis, anoikis, entosis, paraptosis, pyroptosis, ferroptosis,

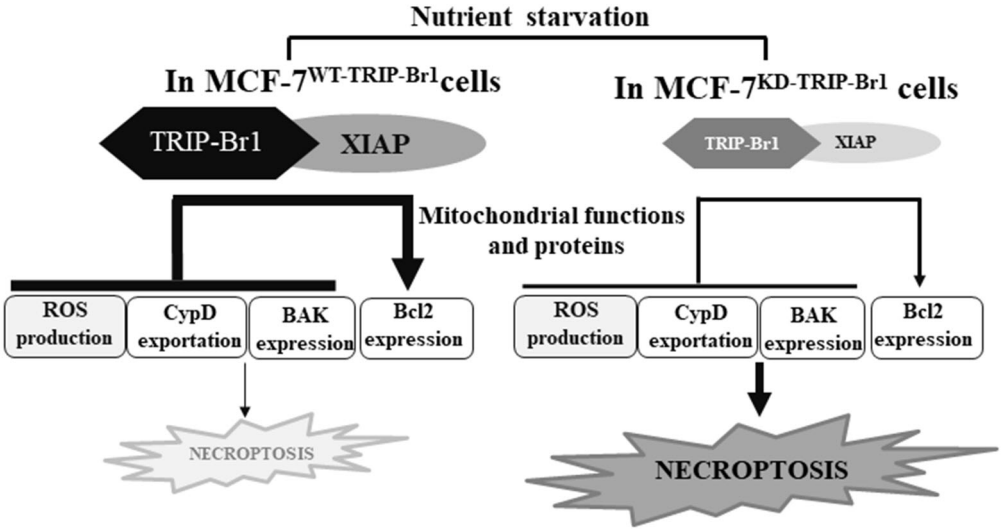

Fig. 7. Summary model. Among the various biological functions of TRIP-Br1 and XIAP in cancer cells, current data suggest that TRIP-Br1 and XIAP inhibit necroptosis by regulating the mitochondrial function. The present study showed that a substantially higher level of TRIP-Br1 was detected in apoptosis resistant MCF-7 breast cancer cells under nutrient starved, serum deficiency, and overcrowded conditions. XIAP was further stabilized and XIAP activity was enhanced in MCF-7 cells carrying wild type TRIP-Br1, in which necroptosis was greatly suppressed in response to serum starved condition. Serum starvation-induced TRIP-Br1 accumulated in the mitochondrial matrix and inhibited necroptosis by reducing ROS generation, suppressing CypD exportation into cytosol, repressing BAX expression, and inducing Bcl2 expression. XIAP levels strongly enhanced this effect. We propose a plausible model suggesting that TRIP-Br1/XIAP is an attractive target to trigger necroptosis for efficient killing of cancer cells under low-nutrient conditions, especially in apoptosis-resistant cancer cells such as MCF-7 cells that lack apoptosis and necroptosis machineries. This study suggest that treatment with a necroptotic inducer represents an alternative to chemotherapy in the management of drug resistant cancer.

mitotic catastrophe, and efferocytosis. In addition, mitochondria are strongly involved in most of these types of cell death. Based on the role of TRIP-Br1 in necroptosis and apoptosis and the presence of TRIP-Br1 in mitochondria, it is plausible that TRIP-Br1 regulates several types of cell deaths. A majority of studies investigated the role of XIAP in apoptosis, but not in necroptosis. Our study showed that silencing XIAP accelerated necroptosis. Therefore, it is interesting to determine the mechanism underlying the regulatory role of TRIP-Br1/XIAP in response to different stresses and stimuli (e.g., anti-cancer drug, hypoxia, pH, and temperature) as well as nutrient starvation.

In conclusion, this study demonstrated that TRIP-Br1 and XIAP act as onco-proteins by suppressing necroptosis of cancer cells under nutrient/serum starvation (Fig. 7). Considering the strong inhibitory role of TRIP-Br1/XIAP in serum starvation-mediated necroptosis of cancer cells highly resistant to apoptosis and necroptosis, targeting TRIP-Br1/XIAP represents an alternative strategy of necroptosis activation in cancer cells and can be potential targets in both cancer diagnosis and cancer therapy. Elucidation of its mechanism provides promising therapeutic targets for cancer treatment.

Disclosure

The authors have no potential conflicts of interest to disclose.

ACKNOWLEDGMENTS

The work reported in this paper was supported by a grant (No. NRF- 2016R1A5A1011974) awarded by the National Research Foundation of Korea (NRF) funded by the Korean Government (MSIP).

ORCID

Zolzaya Sandag https://orcid.org/0000-0001-9901-2156
Samil Jung https://orcid.org/0000-0003-1299-9424
Nguyen Thi Ngoc Quynh https://orcid.org/0000-0001-6286-5139
Davaajargal Myagmarjav https://orcid.org/0000-0003-3075-6258
Nguyen Hai Anh https://orcid.org/0000-0002-6085-8880
Dan-Diem Thi Le https://orcid.org/0000-0003-3922-9315
Beom Suk Lee https://orcid.org/0000-0001-8986-7732
Raj Kumar Mongre https://orcid.org/0000-0002-5120-1844
Taeyeon Jo https://orcid.org/0000-0003-2309-3951
MyeongSok Lee https://orcid.org/0000-0002-2434-0048

REFERENCES

Aharoni-Simon, M., Shumiatcher, R., Yeung, A., Shih, A.Z.L., Dolinsky, V.W., Doucette, C.A., and Luciani, D.S. (2016). Bcl-2 regulates reactive oxygen species signaling and a redox-sensitive mitochondrial proton leak in mouse pancreatic β-cells. Endocrinology *157*, 2270-2281.

Belizário, J., Vieira-Cordeiro, L., and Enns, S. (2015). Necroptotic cell death signaling and execution pathway: lessons from knockout mice. Mediators Inflamm. *2015*, 128076.

Berezovskaya, O., Schimmer, A.D., Glinskii, A.B., Pinilla, C., Hoffman, R.M., Reed, J.C., and Glinsky, G.V. (2005). Increased expression of apoptosis inhibitor protein XIAP contributes to anoikis resistance of circulating

human prostate cancer metastasis precursor cells increased expression of apoptosis inhibitor protein XIAPcontributes to anoikis resistance of circul. Cancer Res. *65*, 2378-2386.

Berghe, T., Vanden, Linkermann, A., Jouan-Lanhouet, S., Walczak, H., and Vandenabeele, P. (2014). Regulated necrosis: the expanding network of non-apoptotic cell death pathways. Nat. Rev. Mol. Cell Biol. *15*, 135-147.

Bernardi, P., Krauskopf, A., Basso, E., Petronilli, V., Blalchy-Dyson, E., Di Lisa, F., and Forte, M.A. (2006). The mitochondrial permeability transition from in vitro artifact to disease target. FEBS J. *273*, 2077-2099.

Cai, Z., Jitkaew, S., Zhao, J., Chiang, H.C., Choksi, S., Liu, J., Ward, Y., Wu, L.G., and Liu, Z.G. (2014). Plasma membrane translocation of trimerized MLKL protein is required for TNF-induced necroptosis. Nat. Cell Biol. *16*, 55-65.

Chai, J., Shiozaki, E., Srinivasula, S.M., Wu, Q., Datta, P., Alnemri, E.S., and Shi, Y. (2001). Structural basis of caspase-7 inhibition by XIAP. Cell *104*, 769-780.

Chan, F.K.-M., Luz, N.F., and Moriwaki, K. (2015). Programmed necrosis in the cross talk of cell death and inflammation. Annu. Rev. Immunol. *33*, 79-106.

Christofferson, D.E. and Yuan, J. (2010). Cyclophilin a release as a biomarker of necrotic cell death. Cell Death Differ. *17*, 1942-1943.

Dan, H.C., Sun, M., Kaneko, S., Feldman, R.I., Nicosia, S.V., Wang, H.G., Tsang, B.K., and Cheng, J.Q. (2004). Akt phosphorylation and stabilization of X-linked inhibitor of apoptosis protein (XIAP). J. Biol. Chem. *279*, 5405-5412.

Dasgupta, A., Nomura, M., Shuck, R., and Yustein, J. (2017). Cancer's Achilles' heel: apoptosis and necroptosis to the rescue. Int. J. Mol. Sci. *18*, 1-20.

Dashzeveg, N. and Yoshida, K. (2015). Cell death decision by p53 via control of the mitochondrial membrane. Cancer Lett. *367*, 108-112.

De Almagro, M.C. and Vucic, D. (2015). Necroptosis: pathway diversity and characteristics. Semin. Cell Dev. Biol. *39*, 56-62.

Deveraux, Q.L., Leo, E., Stennicke, H.R., Welsh, K., Salvesen, G.S., Reed, J.C., Boldin, M., Goncharov, T., Goltsev, Y., Wallach, D., et al. (1999). Cleavage of human inhibitor of apoptosis protein XIAP results in fragments with distinct specificities for caspases. EMBO J. *18*, 5242-5251.

Dondelinger, Y., Hulpiau, P., Saeys, Y., Bertrand, M.J.M., and Vandenabeele, P. (2016). An evolutionary perspective on the necroptotic pathway. Trends Cell Biol. *26*, 721-732.

Duckett, C.S., Li, F., Wang, Y., Tomaselli, K.J., Thompson, C.B., and Armstrong, R.C. (1998). Human Iap-like protein regulates programmed cell death downstream of Bcl-X(L) and cytochrome C. Mol. Cell. Biol. *18*, 608-615.

Eigenbrod, T., Park, J.H., Harder, J., Iwakura, Y., and Núñez, G. (2008). Cutting edge: critical role for mesothelial cells in necrosis-induced inflammation through the recognition of IL-1 alpha released from dying cells. J. Immunol. *181*, 8194-8198.

Ferlay, J., Soerjomataram, I., Dikshit, R., Eser, S., Mathers, C., Rebelo, M., Parkin, D.M., Forman, D., and Bray, F. (2015). Cancer incidence and mortality worldwide: sources, methods and major patterns in GLOBOCAN 2012. Int. J. Cancer *136*, E359-E386.

Fulda, S. (2013). The mechanism of necroptosis in normal and cancer cells. Cancer Biol. Ther. *14*, 999-1004.

Geou-Yarh Liou, P.S. (2010). Reactive oxygen species in cancer. Free Radic. Res. *44*, 47-49.

González-Juarbe, N., Gilley, R.P., Hinojosa, C.A., Bradley, K.M., Kamei, A., Gao, G., Dube, P.H., Bergman, M.A., and Orihuela, C.J. (2015). Pore-forming toxins induce macrophage necroptosis during acute bacterial pneumonia. PLoS Pathog. *11*, 1-23.

Halestrap, A.P. (2009). Mitochondria and reperfusion injury of the heart-A holey death but not beyond salvation. J. Bioenerg. Biomembr. *41*, 113-121.

Han, W., Li, L., Qiu, S., Lu, Q., Pan, Q., Gu, Y., Luo, J., and Hu, X. (2007). Shikonin circumvents cancer drug resistance by induction of a necroptotic death. Mol. Cancer Ther. *6*, 1641-1649.

Hanahan, D. and Weinberg, R.A. (2011). Hallmarks of cancer: the next generation. Cell *144*, 646-674.

He, S., Wang, L., Miao, L., Wang, T., Du, F., Zhao, L., and Wang, X. (2009). Receptor interacting protein Kinase-3 determines cellular necrotic response to TNF-α. Cell *137*, 1100-1111.

Hong, S.W., Kim, C.J., Park, W.S., Shin, J.S., Lee, S.D., Ko, S.G., Jung, S.I., Park, I.C., An, S.K., Lee, W.K., et al. (2009). p34SEI-1 inhibits apoptosis through the stabilization of the X-linked inhibitor of apoptosis protein: p34SEI-1 as a novel target for anti-breast cancer strategies. Cancer Res. *69*, 741-746.

Hong, S.W., Shin, J.S., Lee, Y.M., Kim, D.G., Lee, S.Y., Yoon, D.H., Jung, S.Y., Hwang, J.J., Lee, S.J., Cho, D.H., et al. (2011). p34SEI-1 inhibits ROS-induced cell death through suppression of ASK1. Cancer Biol. Ther. *12*, 421-426.

Hsu, S.I.H., Yang, C.M., Sim, K.G., Hentschel, D.M., O'leary, E., and Bonventre, J.V. (2001). TRIP-Br: a novel family of PHD zinc finger- and bromodomain-interacting proteins that regulate the transcriptional activity of E2F-1/DP-1. EMBO J. *20*, 2273-2285.

Izuishi, K., Kato, K., Ogura, T., Kinoshita, T., and Esumi, H. (2000). Remarkable tolerance of tumor cells to nutrient deprivation: possible new biochemical target for cancer therapy. Cancer Res. *60*, 6201-6207.

Jouan-Lanhouet, S., Riquet, F., Duprez, L., Vanden Berghe, T., Takahashi, N., and Vandenabeele, P. (2014). Necroptosis, in vivo detection in experimental disease models. Semin. Cell Dev. Biol. *35*, 2-13.

Jung, S., Li, C., Duan, J., Lee, S., Kim, K., Park, Y., Yang, Y., Kim, K., Lim, J., Cheon, C., et al. (2015). TRIP-Br1 oncoprotein inhibits autophagy, apoptosis, and necroptosis under nutrient/serum-deprived condition. Oncotarget *6*, 29060-29075.

Jung, S., Li, C., Jeong, D., Lee, S., Ohk, J., Park, M., Han, S., Duan, J., Kim, C., Yang, Y., et al. (2013). Oncogenic function of p34SEI-1 via NEDD4-1-mediated PTEN ubiquitination/degradation and activation of the PI3K/AKT pathway. Int. J. Oncol. *43*, 1587-1595.

Jung, S., Ohk, J., Jeong, D., Li, C., Lee, S., Duan, J., Kim, C., Lim, J.S., Yang, Y., Kim, K.I.L., et al. (2014). Distinct regulatory effect of the p34SEI-1oncoprotein on cancer metastasis in HER2/neu-positive and -negative cells. Int. J. Oncol. *45*, 189-196.

Kaczmarek, A., Vandenabeele, P., and Krysko, D.V. (2013). Necroptosis: the release of damage-associated molecular patterns and its physiological relevance. Immunity *38*, 209-223.

Karch, J., Kanisicak, O., Brody, M.J., Sargent, M.A., Michael, D.M., and Molkentin, J.D. (2015). Necroptosis interfaces with MOMP and the MPTP in mediating cell death. PLoS One *10*, 1-12.

Karch, J., Kwong, J.Q., Burr, A.R., Sargent, M.A., Elrod, J.W., Peixoto, P.M., Martinez-Caballero, S., Osinska, H., Cheng, E.H.Y., Robbins, J., et al. (2013). Bax and Bak function as the outer membrane component of the mitochondrial permeability pore in regulating necrotic cell death in mice. Elife *2013*, 1-21.

Kato, K., Tanaka, T., Sadik, G., Baba, M., Maruyama, D., Yanagida, K., Kodama, T., Morihara, T., Tagami, S., OKOCHI, M., et al. (2011). Protein kinase C stabilizes X-linked inhibitor of apoptosis protein (XIAP) through phosphorylation at Ser87 to suppress apoptotic cell death. Psychogeriatrics *11*, 90-97.

Lee, S., Kim, J., Jung, S., Li, C., Yang, Y., Kim, K. I., Lim, J.S., Kim, Y., Cheon, C. Il, and Lee, M.S. (2015). SIAH1-induced p34SEI-1polyubiquitination/degradation mediates p53 preferential vitamin C cytotoxicity. Int. J. Oncol. *46*, 1377-1384.

Lee, S.L.O., Hong, S.W., Shin, J.S., Kim, J.S., Ko, S.G., Hong, N.J., Kim, D.J., Lee, W.J., Jin, D.H., and Lee, M.S. (2009). p34SEI-1 inhibits doxorubicin-induced senescence through a pathway mediated by protein kinase C-delta and c-Jun-NH2-kinase 1 activation in human breast cancer MCF7 cells. Mol. Cancer Res. *7*, 1845-1853.

Li, C., Jung, S., Lee, S., Jeong, D., Yang, Y., Kim, K.I., Lim, J., Cheon, C., Kim, C., and Lee, M. (2015). Nutrient/serum starvation derived TRIP-Br3 down-regulation accelerates apoptosis by destabilizing XIAP. Oncotarget *6*, 7522-7535.

Lin, Y., Choksi, S., Shen, H.M., Yang, Q.F., Hur, G.M., Kim, Y.S., Tran, J.H., Nedospasov, S.A., and Liu, Z.G. (2004).Tumor necrosis factor-induced nonapoptotic cell death requires receptor-interacting protein-mediated cellular reactive oxygen species accumulation. J. Biol. Chem. *279*, 10822-10828.

Lindqvist, L.M., Heinlein, M., Huang, D.C.S., and Vaux, D.L. (2014). Prosurvival Bcl-2 family members affect autophagy only indirectly, by inhibiting Bax and Bak. Proc. Natl. Acad. Sci. U. S. A. *111*, 8512-8517.

Marchi, S., Giorgi, C., Suski, J.M., Agnoletto, C., Bononi, A., Bonora, M., De Marchi, E., Missiroli, S., Patergnani, S., Poletti, F., et al. (2012). Mitochondria-ROS crosstalk in the control of cell death and aging. J. Signal Transduct. *2012*, 1-17.

Marshall, K.D. and Baines, C.P. (2014). Necroptosis: is there a role for mitochondria? Front. Physiol. *5*, 1-5.

Mizutani, Y., Nakanishi, H., Li, Y.N., Matsubara, H., Yamamoto, K., Sato, N., Shiraishi, T., Nakamura, T., Mikami, K., Okihara, K., et al. (2007). Overexpression of XIAP expression in renal cell carcinoma predicts a worse prognosis. Int. J. Oncol. *30*, 919-925.

Montero, J., Dutta, C., Van Bodegom, D., Weinstock, D., and Letai, A. (2013). P53 regulates a non-apoptotic death induced by ROS. Cell Death Differ. *20*, 1465-1474.

Moriwaki, K., Bertin, J., Gough, P.J., Orlowski, G.M., and Chan, F.K. (2015). Differential roles of RIPK1 and RIPK3 in TNF-induced necroptosis and chemotherapeutic agent-induced cell death. Cell Death Dis. *6*, e1636.

Newton, K. and Manning, G. (2016). Necroptosis and inflammation. Annu. Rev. Biochem. *85*, 743-763.

Nikoletopoulou, V., Markaki, M., Palikaras, K., and Tavernarakis, N. (2013). Crosstalk between apoptosis, necrosis and autophagy. Biochim. Biophys. Acta - Mol. Cell Res. *1833*, 3448-3459.

Pasparakis, M. and Vandenabeele, P. (2015). Necroptosis and its role in inflammation. Nature *517*, 311-320.

Redza-Dutordoir, M. and Averill-Bates, D.A. (2016). Activation of apoptosis signalling pathways by reactive oxygen species. Biochim. Biophys. Acta - Mol. Cell Res. *1863*, 2977-2992.

Riedl, S.J., Renatus, M., Schwarzenbacher, R., Zhou, Q., Sun, C., Fesik, S.W., Liddington, R.C., and Salvesen, G.S. (2001). Structural basis for the inhibition of caspase-3 by XIAP. Cell *104*, 791-800.

Rohde, K., Kleinesudeik, L., Roesler, S., Löwe, O., Heidler, J., Schröder, K., Wittig, I., Dröse, S., and Fulda, S. (2017). A Bak-dependent mitochondrial amplification step contributes to Smac mimetic/glucocorticoid-induced necroptosis. Cell Death Differ. *24*, 83-97.

Shiozaki, E.N., Chai, J., Rigotti, D.J., Riedl, S.J., Li, P., Srinivasula, S.M., Alnemri, E.S., Fairman, R., and Shi, Y. (2003). Mechanism of XIAP-mediated inhibition of caspase-9. Mol. Cell *11*, 519-527.

Su, Z., Yang, Z., Xie, L., DeWitt, J.P., and Chen, Y. (2016). Cancer therapy in the necroptosis era. Cell Death Differ. *23*, 748-756.

Su, Z., Yang, Z., Xu, Y., Chen, Y., and Yu, Q. (2015). Apoptosis, autophagy, necroptosis, and cancer metastasis. Mol. Cancer *14*, 48.

Sugimoto, M., Nakamura, T., Ohtani, N., Hampson, L., Hampson, I.N., Shimamoto, A., Furuichi, Y., Okumura, K., Niwa, S., Taya, Y., et al. (1999). Regulation of CDK4 activity by a novel CDK4-binding protein, p34(SEI-1). Genes Dev. *13*, 3027-3033.

Tang, D.J., Hu, L., Xie, D., Wu, Q.L., Fang, Y., Zeng, Y., Sham, J.S.T., and Guan, X.Y. (2005). Oncogenic transformation by SEI-1 is associated with chromosomal instability. Cancer Res. *65*, 6504-6508.

Tang, T.C., Sham, J.S.T., Xie, D., Cancer, O., and Lines, C. (2002). Identification of a Candidate Oncogene SEI-1 within a minimal amplified region at 19q13.1 in ovarian cancer cell lines advances in brief identification of a candidate oncogene SEI-1 within a minimal amplified region. Cancer Res. *62*, 7157-7161.

Teng, X., Degterev, A., Jagtap, P., Xing, X., Choi, S., Denu, R., Yuan, J., and Cuny, G.D. (2005). Structure-activity relationship study of novel necroptosis inhibitors. Bioorg. Med. Chem. Lett. *15*, 5039-5044.

Tsujimoto, Y. and Shimizu, S. (2007). Role of the mitochondrial membrane permeability transition in cell death. Apoptosis *12*, 835-840.

Van Themsche, C., Leblanc, V., Parent, S., and Asselin, E. (2009). X-linked inhibitor of apoptosis protein (XIAP) regulates PTEN ubiquitination, content, and compartmentalization. J. Biol. Chem. *284*, 20462-20466.

Vandenabeele, P., Galluzzi, L., Vanden Berghe, T., and Kroemer, G. (2010). Molecular mechanisms of necroptosis: an ordered cellular explosion. Nat. Rev. Mol. Cell Biol. *11*, 700-714.

Vaseva, A.V., Marchenko, N.D., Ji, K., Tsirka, S.E., Holzmann, S., and Moll, U.M. (2012). P53 opens the mitochondrial permeability transition pore to trigger necrosis. Cell *149*, 1536-1548.

Wang, H., Sun, L., Su, L., Rizo, J., Liu, L., Wang, L.F., Wang, F.S., and Wang, X. (2014). Mixed lineage kinase domain-like protein MLKL causes necrotic membrane disruption upon phosphorylation by RIP3. Mol. Cell *54*, 133-146.

Wang, Z., Jiang, H., Chen, S., Du, F., and Wang, X. (2012). The mitochondrial phosphatase PGAM5 functions at the convergence point of multiple necrotic death pathways. Cell *148*, 228-243.

Wang, Z., Kishimoto, H., Bhat-Nakshatri, P., Crean, C., and Nakshatri, H. (2005). TNFα resistance in MCF-7 breast cancer cells is associated with altered subcellular localization of p21CIP1and p27KIP1[4]. Cell Death Differ. *12*, 98-100.

Xu, Y.Z., Kanagaratham, C., Youssef, M., and Radzioch, D. (2016). New frontiers in cancer chemotherapy: targeting cell death pathways. In Cell Biology: New Insights, S. Najman, ed. (Rijeka, Croatia: InTech), pp. 93-140.